

Electroclinic effect in a chiral smectic-A liquid crystal stabilized by an anisotropic polymer network

Mohamed Petit and Abdelylah Daoudi*

Laboratoire de Thermophysique de la Matière Condensée, Equipe de l' UMR-CNRS 8024 Université du Littoral Côte d'Opale, 145, Avenue Maurice Schumann 59140 Dunkerque, France

Mimoun Ismaili and Jean Marc Buisine

Laboratoire de Dynamique et Structure des Matériaux Moléculaires, UMR-CNRS 8024 Université des Sciences et Technologies de Lille, Bâtiment P5, 59655 Villeneuve d'Ascq Cedex, France

(Received 13 September 2006; published 27 December 2006)

We have studied the effect of an anisotropic polymer network on the coupling of molecular tilt to applied electric field in the chiral S_A phase. The polymer network is formed from a photoreactive achiral monomer in a thin planar S_C^* cell. Experimental data, obtained from electro-optical measurements near to the $S_A-S_C^*$ transition temperature, T_c , of the induced molecular tilt, switching time, as well as induced polarization as a function of temperature and electric field strength are presented. The results clearly show that, close to T_c , the electroclinic effect is largely controlled by the polymer network. The experimental results are discussed in the framework of a simple phenomenological model, extended from the Landau model, which includes the bulk free energy arising from the anisotropic interaction between the polymer network and the liquid crystal director, and the elastic free energy resulting from the anchoring (supposed rigid) of the liquid crystal molecules at the polymer boundaries.

DOI: [10.1103/PhysRevE.74.061707](https://doi.org/10.1103/PhysRevE.74.061707)

PACS number(s): 61.30.Hn, 61.41.+e

I. INTRODUCTION

Polymer network stabilized liquid crystals (PSLC) [1,2] have attracted increasing interest over the past decade because of their potential applications mainly in electro-optic devices such as displays and light shutters. The main motivation to incorporate a polymer network in liquid crystal cells was to bulk stabilize a desired director configuration against any mechanical shock and distortions which can irreversibly alter the functionality of the cells. Since earlier studies first performed by Hikmet on polymer network stabilized nematic and smectic-A phases [1,3–5], additional works have concerned materials that consist of cholesteric textures [6–11] or ferroelectric liquid crystals stabilized by an anisotropic network [12–19]. These composite materials consist on a polymer network dispersed in a continuous liquid crystal medium [2,20]. The network is formed by a photochemical cross-linking of small amount (few weight percent) of photoreactive monomers initially dissolved in well aligned liquid crystal cells. When monomers are highly soluble in the liquid crystal, this can lead to the formation of a smooth anisotropic network, with fibril-like structure roughly aligned parallel to the direction initially imposed by the liquid crystal medium in which the network has been formed [5]. On the other hand, it has been demonstrated [21–23] that the polymer network presents some aligning ability on surrounding liquid crystal molecules. This aligning ability is related to surface interactions between the liquid crystal molecules and the network, which in turn imposes its preferred orientation inducing a long-range ordering in the liquid crystal molecular alignment. Therefore, the network

physically influences the properties of the liquid crystal, since it acts as a mechanical field that tends to preserve or to control the orientation of liquid crystal molecules upon application of an electric field [12,18,25,26]. This alignment effect of the network obviously has an influence on electro-optical properties. Previous studies have demonstrated changes in the driving voltage and improvements in response times of nematic cells [25,26], and even some original electro-optical effects of ferroelectric liquid crystal such as gray-scale operation [18,23], or a transformation from bistability to monostability [15,16] have been achieved by the introduction of polymer networks. The electro-optical behaviors of PSLCs are intimately related to the morphology and structural characteristics of the network. To explain the experimental results, a two-dimensional bundle model for the polymer network was proposed [2,24–26]. These models consist on nanosized fibrils formed from a few polymer molecular chains. These fibrils are assembled to form parallel cylindrical bundles with lateral size of a few tenths of microns, randomly distributed within the liquid crystal medium. The average distance between the polymer bundles depends on the polymer concentration, ranging from a few microns to some tenths of micron. A good agreement between the experimental data and these models has been demonstrated [25,26], showing that the electro-optical behaviors of PSLCs are governed by the interaction between the liquid crystal molecules and the polymer network. This interaction has been described in terms of anchoring forces imposed by the polymer bundle surface on the liquid crystal molecules. In this work, we report the switching behavior of the induced molecular tilt, the so-called electroclinic effect, in the chiral S_A phase of a polymer-stabilized ferroelectric liquid crystal. The electroclinic effect, which is a switching mechanism that exists in chiral smectic phases, was found by Garoff and

*Electronic address: daoudi@univ-littoral.fr

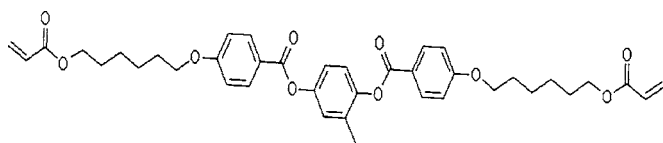


FIG. 1. Molecular structure of the nematogenic diacrylate monomer used in this study.

Meyer [27,28], and results from a direct coupling between the induced molecular tilt and the applied electric field: The application of an electric field parallel to smectic layers induces a free rotation of the molecules perpendicular to the electric field and produces a nonzero average of the transverse component of the molecular polarization. The tilt of the molecular orientation relative to the smectic layer normal is then induced in a plane perpendicular to the induced polarization. We have measured the static and dynamic characteristics of the electroclinic switching in the chiral S_A phase of a ferroelectric liquid crystal. The S_A phase was studied in two planar geometries: The first being stabilized only by the surfaces (SSFLC geometry) and the other by the surfaces and through an anisotropic polymer network. The electro-optical characteristics were measured as a function of electric field strength and temperature and analyzed in the framework of bundle model of the polymer network.

II. EXPERIMENTS

We have used in this study the ferroelectric liquid crystal FLC 8823 (Rolic Research Ltd), which presents on heating the following phase sequence between the crystalline (Cr) and the isotropic liquid (I) phases: Cr— -27°C — S_C^* — -63.5°C — S_A — -65°C — I , where S_C^* denotes the chiral smectic- C phase. To prepare the polymer network we have used a photoreactive diacrylate mesogen as photocurable monomer which presents a nematic (N) phase between Cr and I phases (Cr— 88°C — N — 118°C — I). The chemical structure of the diacrylate monomer used is given in Fig. 1. The photopolymerization was initiated with Irgacure 369, which was added to the monomer with a concentration of 0.5 wt. % (weight percent). The reactive monomer, together with photoinitiator, were dissolved into the liquid crystal in a ratio 5:95 wt. %. This mixture was then inserted in the isotropic state into a $2\ \mu\text{m}$ thick EHC cell (EHC Inc., Japan) coated with ITO (indium tin oxide) and rubbed polyimide, which promotes the formation of planar geometry. The active area was $25\ \mu\text{m}^2$. The cell was then slowly cooled at a $0.1^\circ\text{C}\ \text{min}^{-1}$ cooling rate down to room temperature under an applied electric field of $5\ \text{V}\ \mu\text{m}^{-1}$, 1 Hz to improve the sample alignment. After this procedure, the applied field was switched off, and the cell was irradiated with an ultraviolet light source with an intensity of $5\ \text{mW}\ \text{cm}^{-2}$ at a $\lambda = 365\ \text{nm}$ wavelength during 30 mn to induce polymerization. A SSFLC cell was prepared with the same thermal treatment under applied field than that explained above in order to examine the effect of the polymer network on the electro-optical behaviors of PSFLC samples. The observation of textures was performed by means of a polarized optical micro-

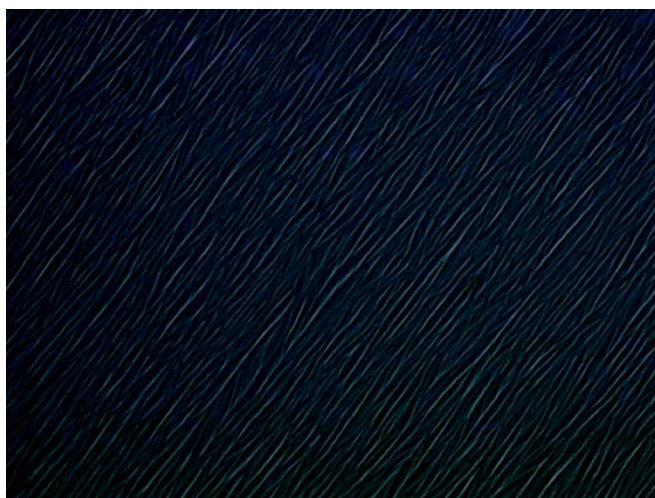


FIG. 2. (Color online) Optical micrograph ($\times 200$) of the PS-FLC sample observed between crossed polarizers in the isotropic phase. The aligning direction was orientated by 45° with respect to polarizer.

scope (LEICA DMRXP) between crossed polarizers. A classical electro-optical setup was used for the measurements of the induced tilt angle, θ , induced polarization, P , and relaxation time, τ_r . Details of measurement techniques have been described elsewhere [29,30]. Measurement accuracies of $\pm 0.5^\circ$, 5%, and 6% were obtained for θ , P , and τ_r , respectively. In our experiments, the sample cell was mounted in a heating-cooling stage Linkam THMSE 600 for temperature control.

III. RESULTS AND DISCUSSION

A. Phase behaviors and optical microscopy structure of the network

The phase behaviors of the PSFLC film are qualitatively the same as that observed for the FLC. The microscopic observation of the texture and texture changes upon heating the PSFLC sample reveals the existence of the S_C^* — S_A and S_A — I phase transitions at temperatures of 63.2°C and 64.2°C , respectively. Note the reduction of the transition temperatures as compared to the pure liquid crystal, since they were shifted to lower temperatures by 0.3°C for the S_C^* — S_A transition and by 0.8°C for the S_A — I transition. Figure 2 shows the texture of the PSFLC film observed at a temperature above the S_A — I transition temperature. Despite the liquid crystal matrix being isotropic, the optical micrograph shows the existence of a longer-ranged ordering structure within the composite film, with long anisotropic stripes preferentially oriented along the rubbing direction. These observed anisotropic stripes are stable and show no aging effects after storing the samples for a few months, and when they are submitted to several heating-cooling cycles; the microscopic observations of these samples has not revealed any noticeable difference in the anisotropic structure of the stripes. We can then conclude from these optical microscopy observations that the striped domains are associated with the

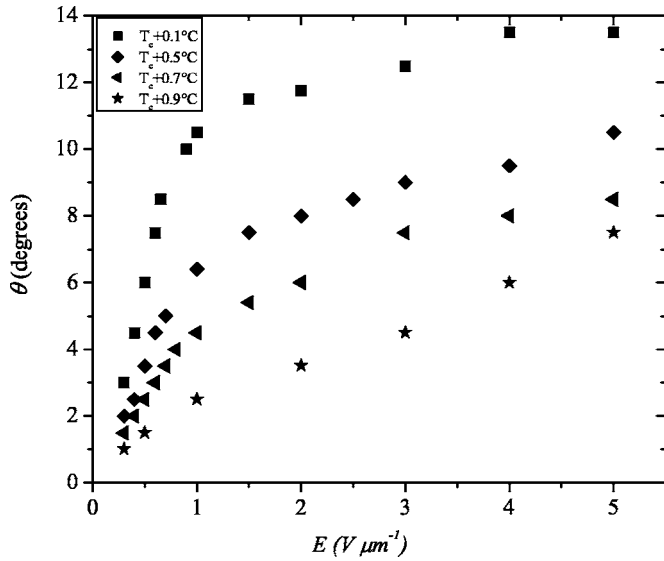


FIG. 3. Induced tilt angle θ in the S_A phase of the FLC sample in surface stabilized geometry as a function of electric field strength and temperature.

polymer network, which is aligned parallel to the rubbing direction, and seems to be separated from the liquid crystal in the form of fibrils.

B. Electroclinic behavior

In Fig. 3 we plot typical examples of the induced tilt angle θ in the S_A phase of the pure FLC in the SSFLC geometry as a function of the applied electric field E at several different temperatures. As reported previously by Lee and Patel [31,32], it can be seen from Fig. 3 that near the $S_C^*-S_A$ transition temperature, T_c , the field induced molecular tilt first linearly increases with E for small fields, then deviates significantly from a linear dependence at moderate fields. For high fields, θ shows a tendency toward saturation. With increasing temperature, the deviation from the linear behavior becomes less pronounced. The dependence of θ with E at different temperatures for the FLC stabilized by the anisotropic polymer network is shown in Fig. 4. It can be seen that $\theta(E)$ of the FLC in the presence of the network shows qualitatively a similar trend that observed for the FLC stabilized by the surfaces (Fig. 3). The most important difference in the behavior of the field induced tilt between the two systems is the magnitude of the variation of θ versus E . For example, at a temperature $T=T_c+0.1$ °C, θ reaches the saturation regime at an electric field of about $1 \text{ V } \mu\text{m}^{-1}$ and saturates at $\theta \approx 13^\circ$ for the SSFLC cell; whereas for the PSFLC cell, this regime was reached at a field of about $2 \text{ V } \mu\text{m}^{-1}$ and θ saturated at $\approx 10^\circ$. To characterize more quantitatively the electroclinic behavior of the two systems, we shall focus our attention below only on the linear parts of $\theta(E)$ plots, at a relatively small field regime. It will be convenient here to introduce the electroclinic coefficient:

$$e_c(T) = \frac{\theta}{E}, \quad (1)$$

which defines the variation rate of θ versus E at small fields, i.e., in linear regime, and at a temperature T . The values of e_c

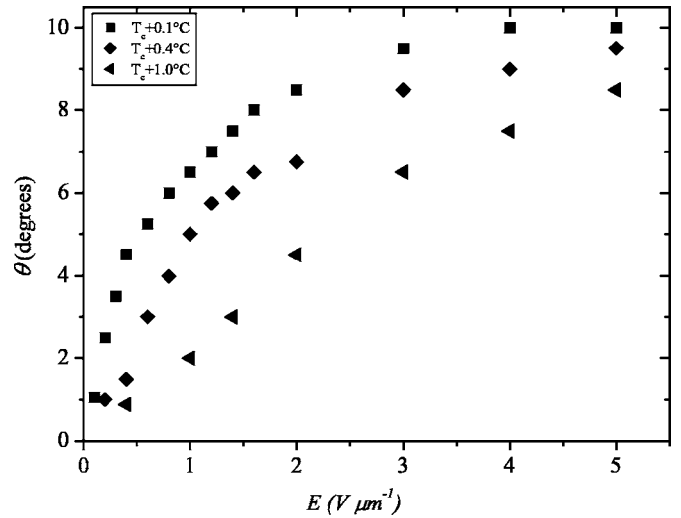


FIG. 4. Induced tilt angle θ in the S_A phase of the polymer-stabilized FLC sample as a function of the electric field strength and temperature.

were then calculated according to Eq. (1) at all studied temperatures for the two systems. Figure 5 is a plot of e_c as a function of $T-T_c$ for SSFLC and PSFLC samples. Clearly for the two systems, e_c decreases rapidly with increasing temperature just above T_c , then shows a weak temperature dependence relatively far from the transition. The behavior of e_c with temperature seems to be consistent with the mean-field model of the electroclinic effect [27,28], which predicts that e_c is simply proportional to the reciprocal reduced temperature $(T-T_c)^{-1}$. As we have mentioned above, there is however a difference on the e_c values between SSFLC and PSFLC samples, mostly in the vicinity of T_c where e_c in the SSFLC cell is larger than that corresponding to the PSFLC one, while it exhibits a tendency to become identical for the two systems as temperature increases. The less pronounced

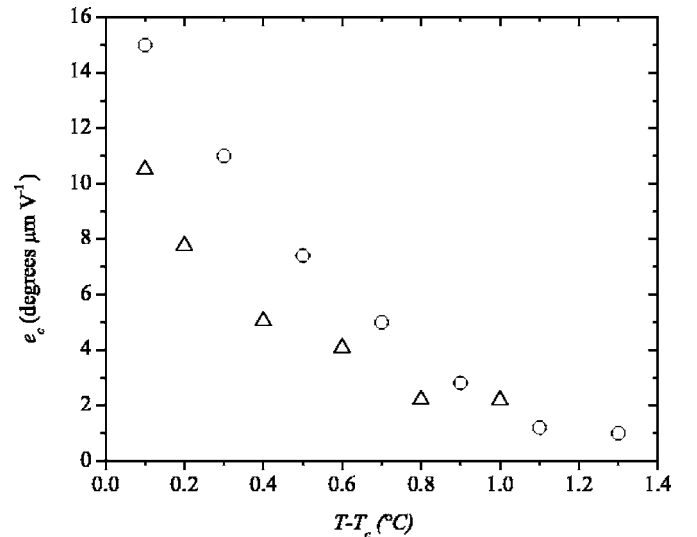


FIG. 5. Plots of the electroclinic coefficient e_c versus temperature $T-T_c$ for surface-stabilized FLC (\circ) and polymer network-stabilized FLC (Δ) cells.

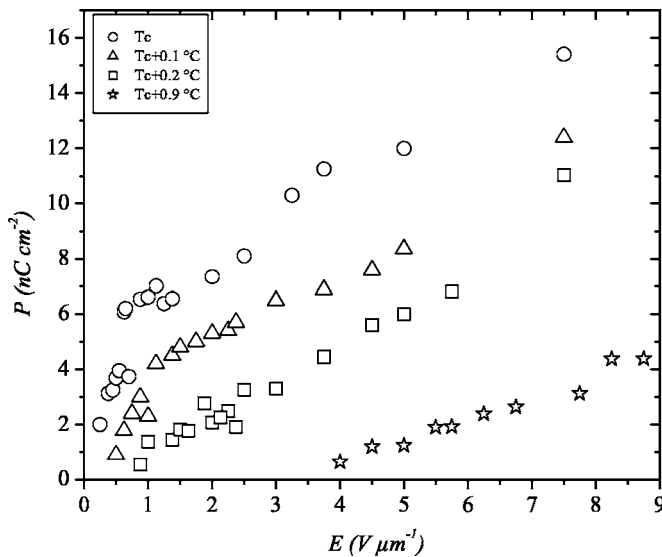


FIG. 6. The induced polarization in the S_A phase of the pure FLC as a function of electric field strength and temperature.

electroclinic effect observed for the FLC stabilized by the anisotropic polymer network compared to the FLC stabilized by the surfaces was confirmed by electric measurements of the field induced polarization P in the S_A phase. Figures 6 and 7 show examples of the induced electroclinic polarization measurements versus the applied electric field at various temperatures for FLC and PSFLC cells, respectively. One can observe from these figures that P versus E curves present a trend similar to θ versus E curves, i.e., a linear behavior at small fields followed by a tendency to saturate at higher fields for temperatures in the close vicinity of T_c . The main feature of the field-induced polarization results (Figs. 6 and 7) is that P in the case of the PSFLC sample is less pronounced than that measured for SSFLC cells. For example, at T_c and for $E=1 \text{ V } \mu\text{m}^{-1}$, the induced polarization de-

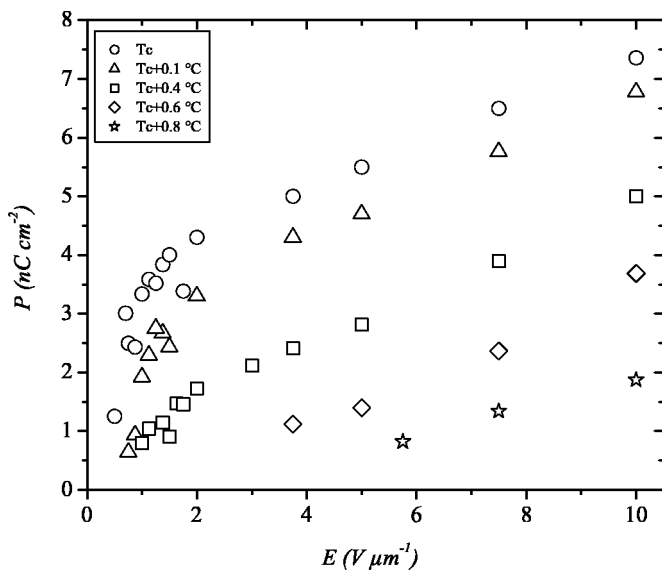


FIG. 7. The induced polarization in the S_A phase of the PSFLC as a function of electric field strength and temperature.

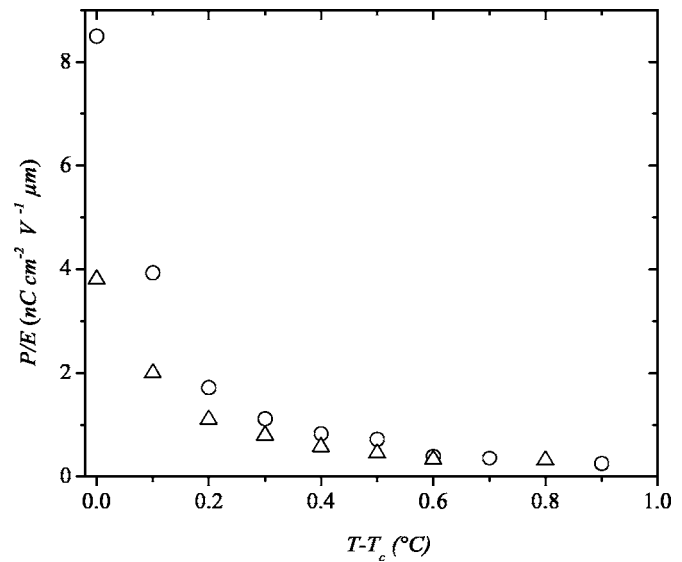


FIG. 8. Plots of P/E versus temperature $T-T_c$ for surface-stabilized FLC (\circ) and polymer network-stabilized FLC (Δ) cells.

creases from $P \approx 7 \text{ nC cm}^{-2}$ for SSFLC to $P \approx 3.5 \text{ nC cm}^{-2}$ for the PSFLC. To illustrate the effect of the polymer network on the field-induced polarization, we plotted in Fig. 8 the electric susceptibility, P/E , corresponding to the linear regime (at low fields), which contains a contribution from the electroclinic susceptibility, as a function of the reduced temperature $T-T_c$. As we can see from Fig. 8, the contribution on P/E arising from the electroclinic susceptibility for both systems is clearly observed, since this contribution is responsible for the rapid increase of P/E when the temperature decreases towards T_c [27,28]. Note that the pretransitional increase of the electric susceptibility $(P/E)(T)$ near T_c is completely consistent with the relatively large values of the electroclinic coefficient observed in the vicinity of T_c (Fig. 5). The fact that the behavior of $(P/E)(T)$ is correlated to that of e_c near T_c is not really a surprising result because the induced electroclinic polarization is linearly coupled to the induced tilt angle [27,28]. Hence the susceptibility measurements provide complimentary data to confirm the electro-optical results. The electroclinic susceptibility of the FLC in surface stabilized geometry is then stronger than that observed when the FLC was stabilized by the polymer network. An opposite behavior has been observed in the vicinity of the $S_C^*-S_A$ transition by Dierking *et al.* [17], i.e., an increase of the polarization when the FLC is stabilized by a polymer network formed well into the S_C^* phase under a dc electric field. Whereas when the polymer network was formed in the nontilted S_A phase, these authors have demonstrated [17] that the polarization is reduced as compared to the pure FLC. They have interpreted these results by a local stabilization, in polymer dominated regions, of the respective phase, in which the polymerization was carried out. According to the same authors [17], this local stabilization is caused by the elastic interaction of the polymer network with the liquid crystal. The electric measurements confirm, for our systems, the tendency of the electroclinic effect to be reduced when the anisotropic polymer network is dispersed

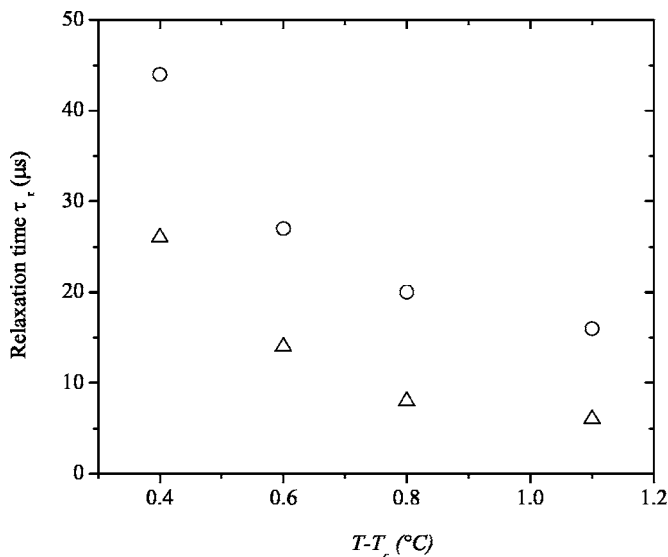


FIG. 9. Plots of the relaxation time τ_r versus temperature $T - T_c$ for surface-stabilized FLC (○) and polymer network-stabilized FLC (△) cells.

within the FLC medium. These results clearly show the influence of the polymer network on the electroclinic response in the S_A phase of the FLC. They also indicate that the network not only stabilizes a preferential alignment of the liquid crystal molecules but also imposes elastic torques that counteract the reorientation of the molecular director when the electric field is applied. The influence of the elastic torques related to the network on the reorientation of the FLC molecules can be considered by another approach. This approach consists of measuring the relaxation dynamics of the electroclinic switching back into the field-off state. By applying successive driving electric pulses to cells, the relaxation time τ_r was measured during the relaxation regime once the electric field was turned off.

In Fig. 9 we plotted τ_r versus $T - T_c$ for SSFLC and PSFLC cells. For the two systems, the measured τ_r seems to follow a $(T - T_c)^{-1}$ law, and clearly shows a critical slowing down of the relaxation when approaching the transition temperature T_c . Furthermore, the interesting feature that Fig. 9 also shows is that the relaxation times of the SSFLC cell are roughly two times slower than those measured for the PSFLC in the temperature range studied. These results agree fairly well with those obtained for the electroclinic coefficient (Fig. 5) and electric susceptibility (Fig. 8), and are coherent with the idea advanced above, according to which the electroclinic switching in the PSFLC system is essentially controlled by the polymer network. All these results clearly indicate that the electroclinic behavior of the FLC is qualitatively similar when the planar alignment of molecules was stabilized either by surfaces or in the bulk through the anisotropic polymer network. However, as we have seen above, a difference on the order of magnitude of the static as well as dynamic characteristics of the electroclinic switching between the two systems has been observed. These quantitative differences are certainly related to the polymer network morphology. It has been already observed by Hikmet *et al.* [5], Dierking *et al.* [8,11], and Held *et al.* [9] that the electro-

optical response of polymer stabilized liquid crystal systems is strongly dependent on the network morphology. For our PSFLC systems, we have demonstrated in Ref. [29] that the helical structure of the short pitch ferroelectric liquid crystal is transferred onto a polymer network during the polymerization process, leading to a twisted morphology of the polymer fibers [Fig. 10(c)]. Due to the anchoring of the liquid crystal molecules on the polymer fibers, this twisted morphology causes elastic forces when the director field distorted upon application of the electric field. In order to examine how the polymer network influences the electroclinic behavior of the FLC, we will develop hereafter a phenomenological model, extended from the mean-field model first developed by Garoff and Meyer, which additionally takes into account not only the structural characteristics of the network, but also the coupling interaction between the FLC and the network.

C. Theoretical framework

Although polymer networks formed in liquid crystal media generally have a complex structure, they have been previously modeled as an assembly of parallel cylinders randomly distributed within the liquid crystal media [2,24–26]. The cylinders are interconnected via a chemical cross linking which ensure the network stability. In the framework of the rigid model of the network introduced by Li *et al.* [18], they considered that FLC molecules are affected by the bulk anchoring force from network. Li *et al.* interpreted this bulk anchoring force in terms of a fieldlike effect, where the orientation of the FLC molecules was coupled to that of the anisotropic polymer network. This model gives a macroscopic description of the polymer network and was successfully applied to describe the “V-shaped” electro-optic properties of FLC gels [18]. We adopt in our theoretical approach this model structure of random polymer network of Li *et al.* We will consider below as a characteristic parameter of the polymer network structure the average intercylinder distance, which we call L_c , and we try to analyze the effect of the applied electric field on smectic- A layers confined between two successive cylinders. The basic relation giving the free energy density of a chiral S_A phase near T_c in the presence of a small electric field E was expressed by Garoff *et al.* [27,28] as

$$f_E = f_0 + \frac{1}{2}\alpha(T - T_0)\theta^2 - CP\theta + \frac{P^2}{2\epsilon_0\chi} - PE. \quad (2)$$

f_0 represents contributions to free energy density from the undistorted S_A phase. α is the mean-field coefficient and C is related to the piezoelectric coupling between the polarization P and the induced electroclinic tilt θ . ϵ_0 is the dielectric constant and χ is the electric susceptibility. Moreover, to the free energy density term expressed in Eq. (2), two other contributions are required to describe the effect of electric field on S_A blocks confined between the polymer fibers. The first one consists of the free energy density f_{ps} arising from the bulk polymer stabilization, and may be written as [18]

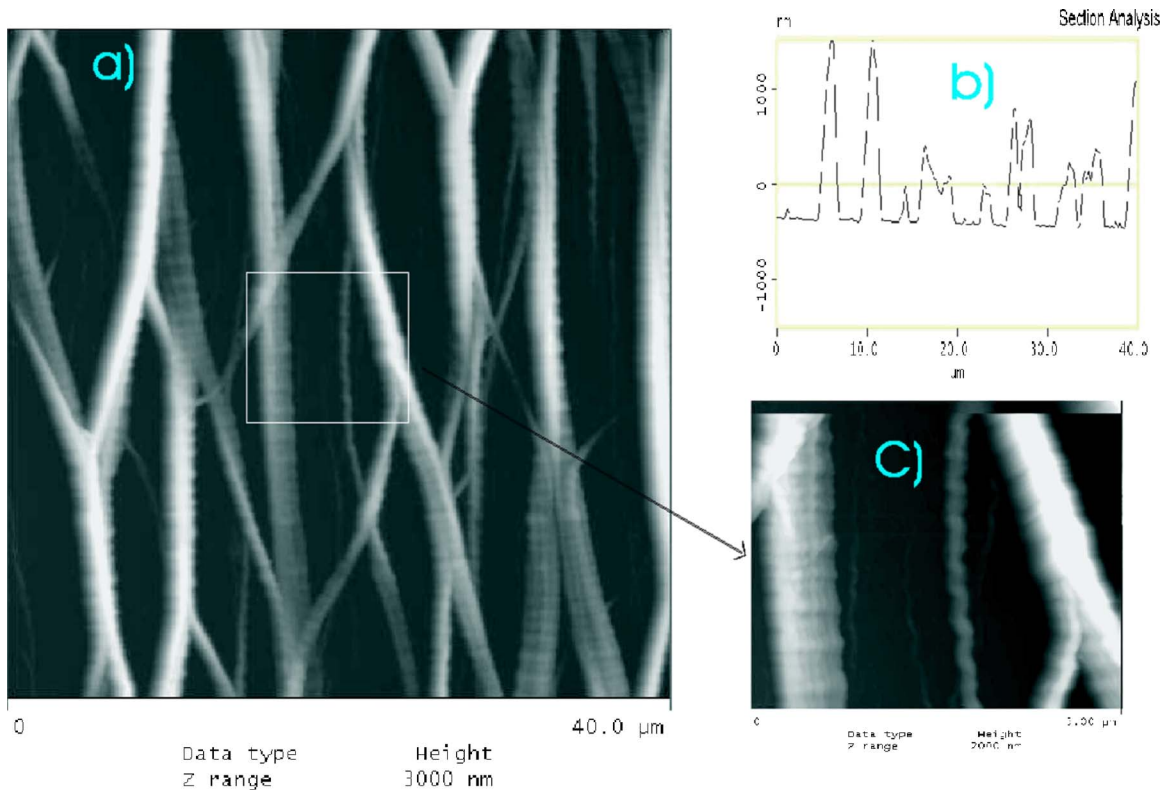


FIG. 10. (Color online) Tapping mode AFM images of polymer network structure of (a) $40 \times 40 \mu\text{m}^2$ and (c) $5 \times 5 \mu\text{m}^2$ regions. Figure (b) corresponds to height profile of the network structure.

$$f_{\text{ps}} = \frac{1}{2} W_p \sin^2 \theta \approx \frac{1}{2} W_p \theta^2. \quad (3)$$

W_p is the coupling coefficient for the interaction between the polymer network and the liquid crystal molecular director. Equation (3) is an approximative expression of f_{ps} because we are interested in low field regime where the θ angle is small. The second contribution comes from the elastic free energy density f_{el} arising from a director distortion upon application of E . In our system, the smectic layers are arranged perpendicular to the direction of the fibers. Between two successive groups of fibers (separated by the average distance L_c), due to anchoring forces between the liquid crystal molecules and the polymer network, the rotation of the director can be reasonably assumed not to be uniform: It is larger at (or close to) $L_c/2$ and weaker near the surface fibers. We must remark here that this theoretical approach of our PS-FLC system is based on a one-dimensional model. We neglect then any splay deformation of the director, and we only consider the elastic energy arising from a twist deformation. f_{el} can then be given by the following expression:

$$f_{\text{el}} = \frac{1}{2} K_2 \left(\frac{\partial \theta}{\partial z} \right)^2, \quad (4)$$

where K_2 is the twist elastic constant and z denotes the coordinate along the axis parallel to the direction of the applied electric field. The total free energy density $f_i = f_E + f_{\text{el}} + f_{\text{ps}}$ is then expressed as

$$f_i = f_0 + \frac{1}{2} \alpha (T - T_0) \theta^2 - CP\theta + \frac{P^2}{2\epsilon_0\chi} - PE + \frac{1}{2} W_p \theta^2 + \frac{1}{2} K_2 \left(\frac{\partial \theta}{\partial z} \right)^2. \quad (5)$$

The equilibrium values of P and θ are found by minimizing the free energy f_i with respect to P and θ , respectively. This leads to the following equations:

$$\alpha(T - T_0)\theta - CP + W_p\theta - K_2 \frac{\partial^2 \theta}{\partial z^2} = 0, \quad (6)$$

$$C\theta - \frac{P}{\epsilon_0\chi} + E = 0. \quad (7)$$

Inserting Eq. (7) into Eq. (6) gives

$$K_2 \frac{\partial^2 \theta}{\partial z^2} - \alpha(T - T'_c)\theta + C\epsilon_0\chi E = 0, \quad (8)$$

where $T'_c = T_c - W_p/\alpha$ is the $S_C^* - S_A$ transition temperature of the PSFLC system; $T_c = T_0 + C^2\chi\epsilon_0/\alpha$ is the $S_C^* - S_A$ transition temperature of pure FLC. Equation (8) governing the director distortion induced by an applied electric field in the S_A phase is analogous to that describing the director profile in the TGB_A phase; the S_A blocks are confined between screw dislocation lines [33]. The analogy comes from the idea that the anisotropic polymer fibers in PSFLC systems constrain the molecular orientation at their surfaces as the screw dis-

locations at the grain boundaries in the TGB_A phase do. To solve Eq. (8), we assume the anchoring of the molecules at the fiber surfaces to be rigid. The boundary conditions at these surfaces are

$$\theta(z=0) = \theta(z=L_c) = 0. \quad (9)$$

Equation (8) has a solution:

$$\theta(z) = \frac{\epsilon_0 \chi C E}{\alpha(T-T'_c)} \left[1 - \frac{\exp(z/a)}{1 + \exp(L_c/a)} - \frac{\exp(-z/a)}{1 + \exp(-L_c/a)} \right], \quad (10)$$

where

$$a = \sqrt{\frac{K_2}{\alpha(T-T'_c)}}. \quad (11)$$

Averaging the $\theta(z)$ values over the $0 \leq z \leq L_c$ domain gives the expression of the mean induced tilt:

$$\langle \theta \rangle = \frac{\epsilon_0 \chi C E}{\alpha(T-T'_c)} \left[1 - \frac{\tanh(L_c/2a)}{(L_c/2a)} \right], \quad (12)$$

which leads to the expression of the electroclinic coefficient, e_c^{PSFLC} , of the polymer-stabilized FLC cell:

$$e_c^{\text{PSFLC}} = \frac{\langle \theta \rangle}{E} = \frac{\epsilon_0 \chi C}{\alpha(T-T'_c)} \left[1 - \frac{\tanh(L_c/2a)}{(L_c/2a)} \right]. \quad (13)$$

For a non-polymer-stabilized FLC cell, the expression of the electroclinic coefficient, e_c^{FLC} , is given by [27,28]

$$e_c^{\text{FLC}} = \frac{\epsilon_0 \chi C}{\alpha(T-T_c)}. \quad (14)$$

T_c is the $S_C^* - S_A$ transition temperature of pure FLC. Comparing Eq. (13) to Eq. (14) for the same given reduced temperature gives

$$\frac{e_c^{\text{PSFLC}}}{e_c^{\text{FLC}}} = 1 - \frac{\tanh(L_c/2a)}{(L_c/2a)}. \quad (15)$$

Equation (15) clearly shows that the presence of the polymer network reduces the field-induced tilt susceptibility of PSFLC samples compared to that of pure FLC film. This effect originates from the anchoring of FLC molecules at surface boundaries of polymer fibers of the network, characterized by a mean distance, L_c , between adjacent fibers. Using our experimental data, it is possible to evaluate from Eq. (15) the characteristic distance L_c . To do that, we must first calculate the mean-field coefficient α to determine the characteristic length a . For this calculation, we reasonably assume, for the pure FLC, that the induced susceptibility

$$\frac{P^{\text{FLC}}}{E} \approx \epsilon_0 \chi C e_c^{\text{FLC}}, \quad (16)$$

where we have taken into account only the electroclinic contribution to the induced polarization and neglected the dielectric component. Using Eq. (14) and Eq. (16) then gives the expression of the mean-field coefficient α of the FLC:

$$\alpha = \frac{P^{\text{FLC}}/E}{(e_c^{\text{FLC}})^2(T-T_c)}. \quad (17)$$

The values of α and a were evaluated at $T-T_c=0.1$ °C according to experimental data in Figs. 5 and 8 and using Eq. (11) and Eq. (17). With a reasonable value of the twist elastic constant, typically $K_2 \approx 10^{-11}$ N, we find $\alpha \approx 5.84 \times 10^{+3}$ N m⁻² K⁻¹ and $a \approx 0.13$ μm. The value of α calculated here is up to one order of magnitude smaller than the values $\alpha \approx (20-50) \times 10^{+3}$ N m⁻² K⁻¹ reported for some FLC compounds [32,34-36], but compare well with the values $\alpha \approx (6-7) \times 10^{+3}$ N m⁻² K⁻¹ obtained by Glogarova *et al.* [38] and Hmine *et al.* [37] for other compounds. With the value of the parameter a calculated above and data of Fig. 5, Eq. (15) was graphically resolved to evaluate L_c . We obtain a mean interfiber distance $L_c \approx 860$ nm. This calculated value is in agreement with that measured by means of Atomic Force Microscope (AFM) experiments (Veeco Instrument Inc.). The tapping mode AFM image of a 40×40 μm² region of the polymer network and the corresponding height profile are presented in Fig. 10. This figure shows a striped structure of the polymer network, with stripes well aligned along the rubbing direction. We can distinguish from the height profile two successive groups of fibers. The average distance between them was evaluated to about 920 nm, which is in accordance with the calculated value. It is also possible to give an estimation of the coupling coefficient, W_p , characterizing the interaction energy between the FLC and the polymer network, from the shift $\Delta T_c = T_c - T'_c = W_p/\alpha$ of the $S_C^* - S_A$ transition temperature. With $\Delta T_c = 0.3$ °C, we find $W_p = 1.75 \times 10^{+3}$ J m⁻³. This value of W_p is higher than values (10-80 J m⁻³) reported by Dierking *et al.* [16,17] in some other PSFLC systems, and is within the order of magnitude than those reported by Furue *et al.* [15] and Li *et al.* [18]. In our earlier studies [29], we have found $W_p \approx 6 \times 10^{+3}$ J m⁻³, which is higher than that found here. This difference is certainly due to a temperature effect, since the value of W_p reported in [29] has been calculated at room temperature, whereas the W_p value found here was evaluated at relatively higher temperature (63.2 °C). The dependence of the anchoring energy on temperature has already been reported by Erdmann *et al.* [39]. These authors have demonstrated that in PDLC systems the anchoring energy decreases when the temperature increases.

IV. CONCLUSION

We have studied the electroclinic effect in the S_A phase of a ferroelectric liquid crystal stabilized by an anisotropic polymer network. Measurements of the field-induced tilt angle, induced polarization, and relaxation time were performed in thin planar cells of the FLC stabilized either by the surfaces or in the bulk by the anisotropic polymer network. We have demonstrated that close to T_c the electroclinic susceptibility as well as the dynamic of the electroclinic switching are largely controlled by the polymer network. The AFM analysis of the network structure has revealed a fibrillar and anisotropic morphology; the polymer fibers present a twisted structure which was printed during the polymerization pro-

cess. This structure of the polymer network imposes a well-defined alignment of the liquid crystal medium along the rubbing direction and, consequently, stabilizes the S_A order. In order to describe how the polymer network influences the electroclinic effect in the chiral S_A phase, we have adopted a one-dimensional model extended from a Landau model initially developed by Garoff *et al.* This model takes into account both the anchoring interaction between the polymer network and the liquid crystal, and the elastic energy due to the distortion of the liquid crystal medium in the presence of an applied electric field. From our experimental data and this theoretical model, an estimate of the anchoring strength yields a value within an order of magnitude of values already reported in the literature. According to this estimated value,

the anchoring interaction between the polymer network and the FLC can be qualified as strong. The characteristic length scale of the polymer network, which defines the average distance between successive fibers, was also calculated and found to be in full agreement with that measured by means of AFM experiments.

ACKNOWLEDGMENTS

The authors would like to thank Dr. Antonio Da Costa from the Laboratoire de Physico-Chimie des Interfaces et Applications of the Université d'Artois-France for assistance in AFM experiments. This research was mainly supported by the EU Program Interreg III "Intelsurf."

-
- [1] D. Broer, R. Gossink, and R. A. M. Hikmet, *Angew. Makromol. Chem.* **183**, 45 (1990).
- [2] *Liquid Crystals in Complex Geometries Formed by Polymer and Porous Networks*, edited by G. P. Crawford and S. Žumer (Taylor & Francis, London, 1996).
- [3] R. A. M. Hikmet, *Liq. Cryst.* **9**, 405 (1991).
- [4] R. A. M. Hikmet and R. Howard, *Phys. Rev. E* **48**, 2752 (1993).
- [5] R. A. M. Hikmet and H. M. J. Boots, *Phys. Rev. E* **51**, 5824 (1995).
- [6] J. W. Doane, D. K. Yang, and M. Pfeiffer, *Macromol. Symp.* **96**, 51 (1995).
- [7] D. J. Deyer, U. P. Schröder, K. P. Chan, and R. J. Twieg, *Chem. Mater.* **9**, 1665 (1997).
- [8] I. Dierking, L. L. Kosbar, A. Afzali Ardakani, A. C. Lowe, and G. A. Held, *J. Appl. Phys.* **81**, 3007 (1997).
- [9] G. A. Held, L. L. Kosbar, I. Dierking, A. C. Lowe, G. Grinstein, V. Lee, and R. D. Miller, *Phys. Rev. Lett.* **79**, 3443 (1997).
- [10] I. Dierking, L. L. Kosbar, A. Afzali Ardakani, A. C. Lowe, and G. A. Held, *Appl. Phys. Lett.* **71**, 2454 (1997).
- [11] I. Dierking, L. L. Kosbar, A. C. Lowe, and G. A. Held, *Liq. Cryst.* **24**, 397 (1998).
- [12] R. A. M. Hikmet, H. M. J. Boots, and M. Michielsen, *Liq. Cryst.* **19**, 65 (1995).
- [13] C. A. Guymon, E. N. Hoggan, D. M. Walba, N. A. Clark, and C. N. Bowman, *Liq. Cryst.* **19**, 719 (1995).
- [14] C. A. Guymon, L. A. Dougan, P. J. Martens, N. A. Clark, D. M. Walba, and C. N. Bowman, *Chem. Mater.* **10**, 2378 (1998).
- [15] H. Furue, T. Takahashi, and S. Kobayashi, *Jpn. J. Appl. Phys., Part 1* **38**, 5660 (1999).
- [16] T. Takahashi, T. Umeda, H. Furue, and S. Kobayashi, *Jpn. J. Appl. Phys., Part 1* **38**, 5991 (1999).
- [17] I. Dierking, M. A. Osipov, and S. T. Lagerwall, *Eur. Phys. J. E* **2**, 303 (2000).
- [18] J. Li, X. Zhu, L. Xuan, and X. Huang, *Ferroelectrics* **277**, 85 (2002).
- [19] E. R. Beckel, N. B. Cramer, A. W. Harant, and C. N. Bowman, *Liq. Cryst.* **30**, 1343 (2003).
- [20] Y. K. Fung, D. K. Yang, S. Ying, L. C. Chien, S. Žumer, and J. W. Doane, *Liq. Cryst.* **19**, 797 (1995).
- [21] G. P. Crawford, A. Scharkowski, Y. K. Fung, J. W. Doane, and S. Žumer, *Phys. Rev. E* **52**, R1273 (1995).
- [22] C. Chiccoli, P. Pasini, G. Skačej, C. Zannoni, and S. Žumer, *Phys. Rev. E* **65**, 051703 (2002).
- [23] H. Furue, Y. Iimura, H. Hasebe, H. Takatsu, and S. Kobayashi, *Mol. Cryst. Liq. Cryst. Sci. Technol., Sect. A* **317**, 259 (1998).
- [24] Y. K. Fung, A. Borštnik, S. Žumer, D. K. Yang, and J. W. Doane, *Phys. Rev. E* **55**, 1637 (1997).
- [25] R. Q. Ma and D. K. Yang, *Phys. Rev. E* **61**, 1567 (2000).
- [26] P. A. Kosyrev, J. Qi, N. V. Priezjev, R. A. Pelcovits, and G. P. Crawford, *Appl. Phys. Lett.* **81**, 2986 (2002).
- [27] S. Garoff and R. B. Meyer, *Phys. Rev. Lett.* **38**, 848 (1977).
- [28] S. Garoff and R. B. Meyer, *Phys. Rev. A* **19**, 338 (1979).
- [29] M. Petit, A. Daoudi, M. Ismaili, and J. M. Buisine, *Eur. Phys. J. E* **20**, 327 (2006).
- [30] K. Miyasato, S. Abe, H. Takezoe, A. Fukuda, and E. Kuze, *Jpn. J. Appl. Phys., Part 1* **22**, 661 (1983).
- [31] S. D. Lee and J. S. Patel, *Appl. Phys. Lett.* **54**, 1653 (1989).
- [32] S. D. Lee and J. S. Patel, *Appl. Phys. Lett.* **55**, 122 (1989).
- [33] M. Ismaili, F. Bougrioua, N. Isaert, C. Legrand, and H. T. Nguyen, *Phys. Rev. E* **65**, 011701 (2001).
- [34] G. Andersson, I. Dahl, W. Kuczynski, S. T. Lagerwall, K. Skarp, and B. Stebler, *Ferroelectrics* **84**, 285 (1988).
- [35] L. Dupont, M. Glogarova, J. P. Marcerou, H. T. Nguyen, C. Destrade, and L. Lejček, *J. Phys. II* **1**, 831 (1991).
- [36] F. Gießelmann and P. Zugenmaier, *Phys. Rev. E* **52**, 1762 (1995).
- [37] J. Hmine, C. Legrand, N. Isaert, and H. T. Nguyen, *Liq. Cryst.* **30**, 227 (2002).
- [38] M. Glogarova and J. Pavel, *Liq. Cryst.* **6**, 325 (1989).
- [39] J. H. Erdmann, S. Žumer, and J. W. Doane, *Phys. Rev. Lett.* **64**, 1907 (1990).